

Solution processed reduced graphene oxide ultraviolet detector

Basant Chitara, S. B. Krupanidhi, and C. N. R. Rao

Citation: *Appl. Phys. Lett.* **99**, 113114 (2011); doi: 10.1063/1.3640222

View online: <http://dx.doi.org/10.1063/1.3640222>

View Table of Contents: <http://apl.aip.org/resource/1/APPLAB/v99/i11>

Published by the [American Institute of Physics](#).

Related Articles

Photoconductive gain in solar-blind ultraviolet photodetector based on Mg_{0.52}Zn_{0.48}O thin film
Appl. Phys. Lett. **99**, 242105 (2011)

High performance single In₂Se₃ nanowire photodetector
Appl. Phys. Lett. **99**, 243105 (2011)

Electrically tuneable spectral responsivity in gated silicon photodiodes
Appl. Phys. Lett. **99**, 231104 (2011)

Infrared photocurrent with one- and two-photon absorptions in a double-barrier quantum well system
J. Appl. Phys. **110**, 104313 (2011)

Solar blind metal-semiconductor-metal ultraviolet photodetectors using quasi-alloy of B_{GaN}/Ga_N superlattices
Appl. Phys. Lett. **99**, 221101 (2011)

Additional information on *Appl. Phys. Lett.*

Journal Homepage: <http://apl.aip.org/>

Journal Information: http://apl.aip.org/about/about_the_journal

Top downloads: http://apl.aip.org/features/most_downloaded

Information for Authors: <http://apl.aip.org/authors>

ADVERTISEMENT

The logo for AIP Advances features the text 'AIP Advances' in a blue and green font. Above the text is a decorative graphic of several orange and yellow circles of varying sizes, some connected by a dotted line, suggesting a molecular or atomic structure.

Submit Now

**Explore AIP's new
open-access journal**

- **Article-level metrics
now available**
- **Join the conversation!
Rate & comment on articles**

Solution processed reduced graphene oxide ultraviolet detector

Basant Chitara,¹ S. B. Krupanidhi,^{1,a)} and C. N. R. Rao^{1,2,a)}

¹Materials Research Centre, Indian Institute of Science, Bangalore 560012, India

²International Centre for Materials Science and CSIR Centre for Excellence in Chemistry, Jawaharlal Nehru Centre for Advanced Scientific Research, Jakkur, P. O., Bangalore 560064, India

(Received 27 June 2011; accepted 26 August 2011; published online 16 September 2011)

Electronic properties of graphene have been studied more extensively than its photonic applications, in spite of its exciting optical properties. Recent results on solar cells, light emitting diodes and photodetectors show its true potential in photonics and optoelectronics. Here, we have explored the use of reduced graphene oxide as a candidate for solution processed ultraviolet photodetectors. UV detection is demonstrated by reduced graphene oxide in terms of time resolved photocurrent as well as photoresponse. The responsivity of the detectors is found to be 0.12 A/W with an external quantum efficiency of 40%. © 2011 American Institute of Physics. [doi:10.1063/1.3640222]

Graphene is a two-dimensional material composed of layers of carbon atoms forming six membered rings. Its high Fermi velocity with linear energy dispersion relation and an extremely high electrical mobility make it an important material for future technologies.^{1–7} These unusual electronic properties of graphene sheets have attracted much attention during the past few years.^{8–13} In addition, it remarkably absorbs $\sim 2\%$ of incident light over a broad wavelength range.^{1–4} The electronic structure and properties of multi-layer graphene depends on the number of layers. Moreover, multilayers absorb additively above ~ 0.5 eV, thereby resulting in strong graphene light interaction. Single or few layer graphenes possessing large areas have already been used as photodetectors.^{3,4,13} Currently, high quality graphene sheets are mostly produced by mechanical exfoliation. However, lower yield of this approach to produce high quality graphene and complications in device applications inhibit their applications in optoelectronics.¹⁴ In addition, large scale synthesis of graphene sheets is also advantageous for their applications in mechanically robust composites,^{15,16} transparent and electrically conductive films.¹⁷ Therefore, considerable amount of interest has been triggered in few-layer graphenes. To address this, graphene oxide (GO) has emerged as a cost effective precursor for bulk production of graphene based materials, wherein the basal plane carbon atoms are decorated with epoxide and hydroxyl groups and the edge atoms bear carbonyl and carboxyl groups.^{18–20} These functional groups impart hydrophilic character by reducing the inter-plane forces, ultimately helping in complete exfoliation of single GO layers in aqueous media. A large portion of oxygen containing functional groups can be removed by the strong chemical reducing agent hydrazine upon deoxygenation of GO.^{21,22} Moreover, optoelectronic properties of GO can be tuned by controlled reduction through chemical or thermal processes. Solution processed thin films of GO provide ease of fabrication at relatively lower costs with mechanical flexibility and their compatibility with various substrates make them suitable for large area device applications. Although, in comparison to graphene, fully reduced

sheets have less room temperature conductivity and carrier mobility, but their solution processability over large areas offers new direction in flexible optoelectronics. In this report, we present the chemically reduced graphene oxide as a suitable candidate for solution processed UV detector. The devices were fabricated by simply dropcasting the reduced graphene oxide (RGO) suspension over glass ultimately paving the path for cost effective optoelectronic devices.

Reduced graphene oxide sheets dispersible in N,N-dimethylformamide (DMF) were synthesised by using the method of Park *et al.*²² Briefly, graphene oxide suspension was produced by sonicating GO followed by the addition of DMF to produce a quite stable light-brown suspension of graphene oxide sheets. Consequently, these sheets were chemically reduced by using hydrazine monohydrate for 12 h at 80 °C, resulting in a homogeneous black suspension. Raman spectra were recorded with LabRAM HR high resolution Raman spectrometer (Horiba Jobin Yvon) using a He–Ne laser (632.8 nm). TEM images were obtained with a JEOL JEM 3010 instrument. Atomic force microscopy (AFM) measurements were performed using a NanoMan instrument. The devices were fabricated by drop casting RGO suspension on pre-cleaned soda lime glass, and the film was dried in vacuum overnight to remove the residual solvent. The electrodes were formed by taking two contacts using silver paste. The separation between the two electrodes was 2 mm and the effective area of the device was ~ 4 mm². Electrical measurements and photoresponse were measured in air using a Keithley 6430 meter. *I-V*

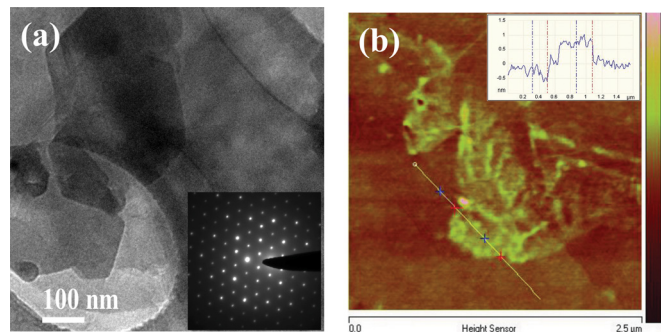


FIG. 1. (Color online) (a) TEM image of reduced graphene oxide and the corresponding ED pattern (shown as an inset). An AFM image is shown in (b) with the height profile as the inset.

^{a)}Authors to whom correspondence should be addressed. Electronic addresses: cnrrao@jncasr.ac.in and sbk@mrc.iisc.ernet.in.

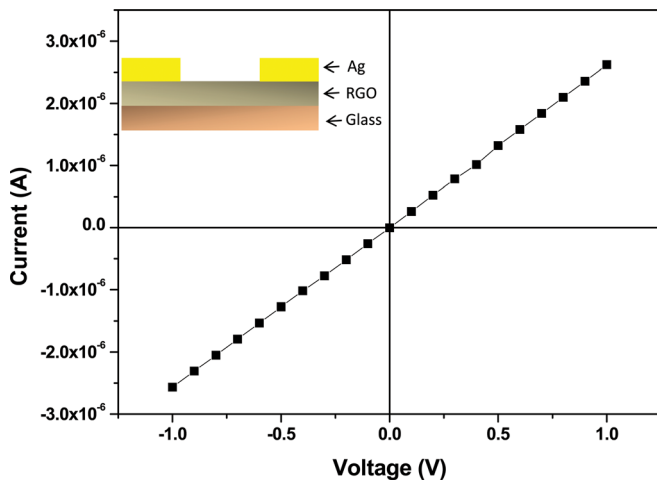


FIG. 2. (Color online) (a) The I - V characteristic of the device (in dark) and the device structure is shown as an inset.

characteristics of the devices were measured in dark and under UV illumination. The UV source consists of a hand held lamp with wavelength of 360 nm with intensity 0.3 mW/cm^2 .

Fig. 1(a) shows the TEM image of reduced graphene oxide and the corresponding electron diffraction (ED) pattern (shown as inset). The ED pattern establishes the presence of hexagonal six-fold symmetry in the sample. The Raman spectrum shows the characteristic D (1320 cm^{-1}) and G bands (1590 cm^{-1}). The 2D-band is absent as reported in the literature. The RGO sample used in the present investigation consists of 1-2 layers as it is evident from the AFM image and corresponding height profile (Fig. 1(b)). Fig. 2 shows the I - V characteristic of the device (in dark) and the device structure is shown as an inset. Fig. 3(a) represents the photo-response for one of the device where the photocurrent is plotted as a function of time with and without UV on the detector. The photocurrent was measured under a bias voltage $V_{\text{bias}} = 1 \text{ V}$. Fig. 3(b) represents the photo-response for one of the device with and without UV on the detector before sat-

uration. In Fig. 3(c), we show the typical I - V characteristics in the dark (squares) and under UV illumination (circles) of the device at 360 nm with 0.3 mW/cm^2 . The UV source was turned on and off to demonstrate the reproducibility of the data with time confirming that the device behaves well under continuous cycling as shown in Fig. 3(d).

Now, we will discuss the mechanism of UV detection in RGO. When the RGO is irradiated with the light, hole and electron pairs are generated.^{23–27} These pairs get separated on the application of an electric field and a photocurrent is generated. As a result, a net increase in current occurs in RGO, leading to detector action. The current start decreasing immediately after switching ON the UV and after sometime, it gets saturated and then started increasing as shown in Fig. 3(a). To investigate this effect further in detail, we have switched on and off the UV light before saturation regime. We observe that the current starts decreasing immediately after switching on UV and reaches its original value after switching off the UV as shown in Fig. 3(b). This can be explained by the fact that the electron trapping of C=O groups in RGO increases at their excited states induced by light radiation.²⁸ Therefore, electron carriers of RGO are largely trapped by oxygenous groups under light radiation, resulting in a decrease of current. Henceforth, the photogenerated electrons are responsible for the increase in current. Thus, the competition between electron trapping by C=O groups and electron photogeneration under light radiation is responsible for the observed behaviour.

Responsivity (R_λ), the ratio of photocurrent generated to the intensity of the incident light on the effective area of a photoconductor,²⁹ and the external quantum efficiency (EQE), defined as the number of electrons detected per incident photon, are two important parameters for the photoconductors. The higher values of R_λ and EQE correspond to high sensitivity. The R_λ and EQE were calculated as $R_\lambda = I_\lambda / (P_\lambda S)$ (Refs. 30 and 31) and $\text{EQE} = hcR_\lambda / (e\lambda)$,^{32,33} where, I_λ represents the photocurrent ($I_{\text{illumination}} - I_{\text{dark}}$), P_λ is the light

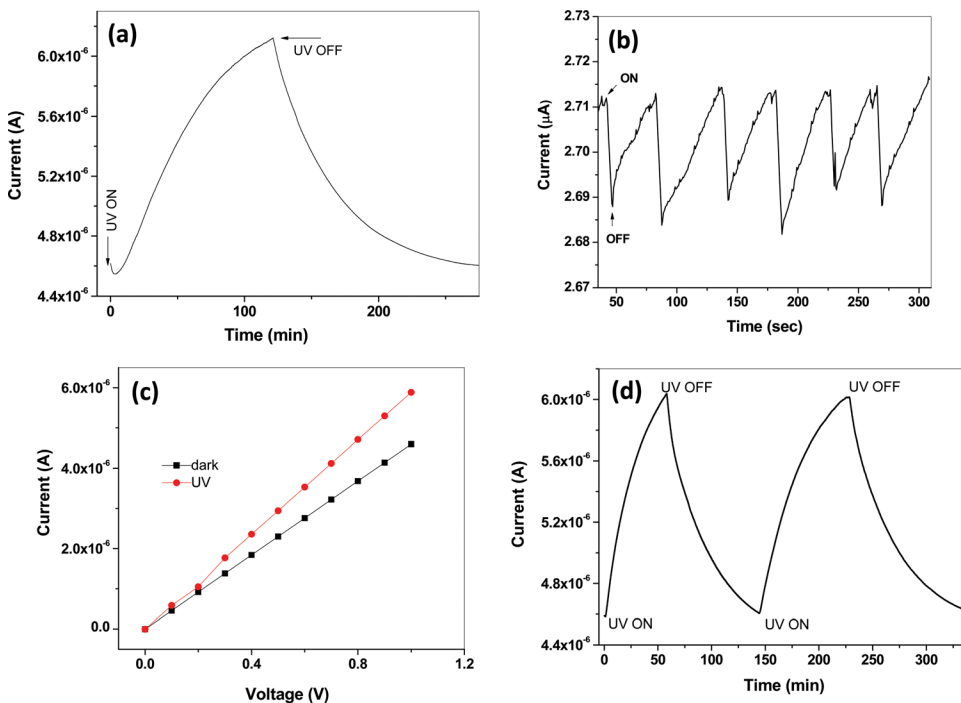


FIG. 3. (Color online) (a) The photo-response for one of the device with and without UV on the detector. The photocurrent was measured under a bias voltage $V_{\text{bias}} = 1 \text{ V}$. (b) The photo-response before saturation. (c) Typical I - V characteristics of the dark (squares) and under UV illumination (circles) of the device at 360 nm with 0.3 mW/cm^2 . The UV source was turned on and off to demonstrate the reproducibility of the data with time as shown in (d).

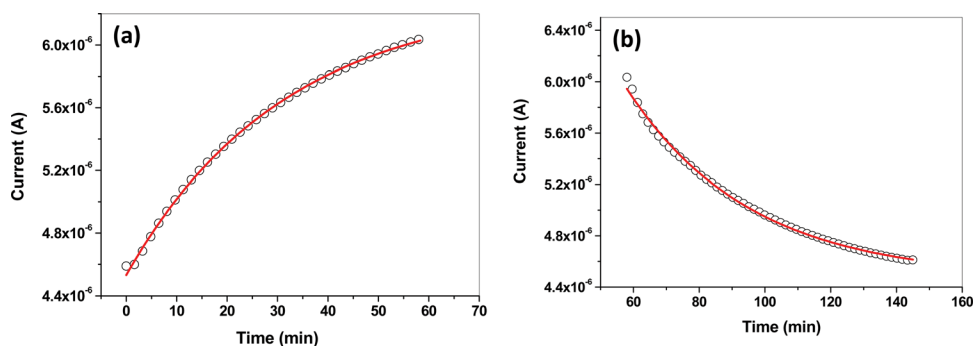


FIG. 4. (Color online) (a) and (b) shows the time response of photocurrent growth and decay for RGO in response to turn on and turn-off of the UV illumination. The open circles are the experimental points and the solid lines are a fit to the equations.

intensity, S is the effective device area under illumination, and λ is the exciting wavelength. From our experimental results, R_{λ} and EQE of RGO are 0.12 A/W and 40%, respectively, for an incident wavelength of 360 nm at 1 V. Thus, these results confirm that RGO is a promising candidate for high-speed nanoscale photodetectors and photoelectronic switches with high selectivity and sensitivity.

It is also worth mentioning about response time, an important factor for photodetectors. Figs. 4(a) and 4(b) show the time response of photocurrent growth and decay for RGO in response to turn on and turn-off of the UV illumination. The photoresponse of our device under UV source can be well described by, Refs. 13 and 34, $I(t) = I_{\text{dark}} + A \{ \exp(t/\tau) \}$ and $I(t) = I_{\text{dark}} + A \{ \exp(-t/\tau) \}$ for growth and decay, respectively, where τ is the time constant, I_{dark} is the dark current, and A is the constant. The open circles are the experimental points and the solid lines are a fit to the above equations. Time constants for growth and decay were estimated to be 30 min and 35 min, respectively. The devices exhibit slow response and recovery times which can be attributed to the competition between electron trapping by C=O groups and electron photogeneration in contrary to conventional metal oxide UV detectors, where UV detection is mainly due to the photogeneration of the carriers where the band gap of active material matches exactly with the energy of the incident radiation, ultimately giving rise to fast response and recovery times. Reproducibility of all results reported here was established by fabricating devices using RGO from different synthesis batches. The devices show no degradation in performance under ambient conditions for over 5 months.

In conclusion, we have demonstrated UV sensing properties of chemically reduced graphene oxide using simple drop cast method. The photodetecting responsivity is found to be 0.12 A/W with an external quantum efficiency of 40%. The competition between electron trapping by C=O groups and electron photogeneration under light radiation is responsible for the observed behaviour.

The authors acknowledge Barun Das for assistance in preparing RGO.

¹R. R. Nair, P. Blake, A. N. Grigorenko, K. S. Novoselov, T. J. Booth, T. Stauber, N. M. R. Peres, and A. K. Geim, *Science* **320**, 1308 (2008).

²F. Wang, Y. Zhang, C. Tian, C. Girit, A. Zettl, M. Crommie, and Y. R. Shen, *Science* **320**, 206 (2008).

³F. Xia, M. Thomas, L. Yu-ming, A. Valdes-Garcia, and P. Avouris, *Nat. Nanotechnol.* **4**, 839 (2009).

⁴M. Thomas, F. Xia, and P. Avouris, *Nature Photon.* **4**, 297 (2010).

⁵K. S. Novoselov, A. K. Geim, S. V. Morozov, D. Jiang, Y. Zhang, S. V. Dubonos, I. V. Grigorieva, and A. A. Firsov, *Science* **306**, 666 (2004).

⁶K. S. Novoselov, A. K. Geim, S. V. Morozov, D. Jiang, M. I. Katsnelson, I. V. Grigorieva, S. V. Dubonos, and A. A. Firsov, *Nature* **438**, 197 (2005).

⁷Y. Zhang, J. W. Tan, H. L. Stormer, and P. Kim, *Nature* **438**, 201 (2005).

⁸P. Avouris, Z. Chen, and V. Perebeinos, *Nat. Nanotechnol.* **2**, 605 (2007).

⁹A. K. Geim and K. S. Novoselov, *Nature Mater.* **6**, 183 (2007).

¹⁰C. N. R. Rao, K. Biswas, K. S. Subrahmanyam, and A. Govindaraj, *J. Mater. Chem.* **19**, 2457 (2009).

¹¹C. N. R. Rao, A. K. Sood, K. S. Subrahmanyam, and A. Govindaraj, *Angew. Chem. Int. Ed.* **48**, 7752 (2009).

¹²C. Berger, Z. M. Song, X. B. Li, X. S. Wu, N. Brown, C. Naud, D. Mayo, T. B. Li, J. Hass, A. N. Marchenkov, E. H. Conrad, P. N. First, and W. A. de Heer, *Science* **312**, 1191 (2006).

¹³S. Ghosh, B. K. Sarker, A. Chunder, L. Zhai, and S. I. Khondaker, *Appl. Phys. Lett.* **96**, 163109 (2010).

¹⁴K. S. Novoselov, D. Jiang, F. Schedin, T. J. Booth, V. V. Khotkevich, S. V. Morozov, and A. K. Geim, *Proc. Natl. Acad. Sci. U.S.A.* **102**, 10451 (2005).

¹⁵S. Stankovich, D. A. Dikin, G. H. B. Dommett, K. M. Kohlhaas, E. J. Zimney, E. A. Stach, R. D. Piner, S. T. Nguyen, and R. S. Ruoff, *Nature* **442**, 282 (2006).

¹⁶D. A. Dikin, S. Stankovich, E. J. Zimney, R. D. Piner, G. H. B. Dommett, G. Evmenenko, S. T. Nguyen, and R. S. Ruoff, *Nature* **448**, 457 (2007).

¹⁷S. Watcharotone, D. A. Dikin, S. Stankovich, R. Piner, I. Jung, G. H. B. Dommett, G. Evmenenko, S. E. Wu, S. F. Chen, C. P. Liu, S. T. Nguyen, and R. S. Ruoff, *Nano Lett.* **7**, 1888 (2007).

¹⁸H. C. Schniepp, J. L. Li, M. J. McAllister, H. Sai, M. Herrera-Alonso, D. H. Adamson, R. K. Prud'homme, R. Car, D. A. Saville, and I. A. Aksay, *J. Phys. Chem. B* **110**, 8535 (2006).

¹⁹A. Lerf, H. Y. He, M. Forster, and J. Klinowski, *J. Phys. Chem. B* **102**, 4477 (1998).

²⁰H. Y. He, J. Klinowski, M. Forster, and A. Lerf, *Chem. Phys. Lett.* **287**, 53 (1998).

²¹S. Stankovich, R. D. Piner, X. Q. Chen, N. Q. Wu, S. T. Nguyen, and R. S. Ruoff, *J. Mater. Chem.* **16**, 155 (2006).

²²S. Park, J. An, I. Jung, R. D. Piner, S. J. An, X. Li, A. Velamakanni, and R. S. Ruoff, *Nano Lett.* **9**, 1593 (2009).

²³F. Yan, P. Migliorato, and R. Ishihara, *Appl. Phys. Lett.* **88**, 153507 (2006).

²⁴S. M. Mok, F. Yan, and H. L. W. Chan, *Appl. Phys. Lett.* **93**, 023310 (2008).

²⁵C. L. Donley, J. Zaumseil, J. W. Andreasen, M. M. Nielsen, H. Sirringhaus, R. H. Friend, and J. S. Kim, *J. Am. Chem. Soc.* **127**, 12890 (2005).

²⁶L. Liu, S. M. Ryu, M. R. Tomasik, E. Stolyarova, N. Jung, M. S. Hybertsen, M. L. Steigerwald, L. E. Brus, and G. W. Flynn, *Nano Lett.* **8**, 1965 (2008).

²⁷X. S. Wu, M. Sprinkle, X. B. Li, F. Ming, C. Berger, and W. A. de Heer, *Phys. Rev. Lett.* **101**, 026801 (2008).

²⁸H. Chang, Z. Sun, Q. Yuan, F. Ding, X. Tao, F. Yan, and Z. Zheng, *Adv. Mater.* **22**, 4872 (2010).

²⁹H. Morkoc, A. D. Carlo, and P. Cingolani, *Solid-State Electron.* **46**, 157 (2002).

³⁰J. P. Cheng, Y. J. Zhang, and R. Y. Guo, *J. Cryst. Growth* **310**, 57 (2008).

³¹T. Ueda, Z. H. An, K. Hirakawa, and S. Komiyama, *J. Appl. Phys.* **103**, 093109 (2008).

³²X. P. Chen, H. L. Zhu, J. F. Cai, and Z. Y. Wu, *J. Appl. Phys.* **102**, 024505 (2007).

³³S. Alamaviva, M. Marinelli, E. Milani, G. Prestopino, A. Tucciarone, C. Verona, G. Verona-Rinati, M. Angelone, and M. Pillon, *Diamond Relat. Mater.* **18**, 101 (2009).

³⁴N. Liu, G. Fang, W. Zeng, H. Zhou, F. Cheng, Q. Zheng, L. Yuan, X. Zou, and X. Zhao, *ACS Appl. Mater. Interfaces* **2**, 1973 (2010).